

# Spreading Shape and Area Regulate the Osteogenesis of Mesenchymal Stem Cells

Yang Zhao<sup>1</sup> · Qing Sun<sup>1</sup> · Shurong Wang<sup>1</sup> · Bo Huo<sup>1</sup> 

Received: 16 June 2019/Revised: 26 July 2019/Accepted: 31 July 2019/Published online: 29 August 2019  
© The Korean Tissue Engineering and Regenerative Medicine Society 2019

## Abstract

**BACKGROUND:** Mesenchymal stem cells (MSCs) have strong self-renewal ability and multiple differentiation potential. Some studies confirmed that spreading shape and area of single MSCs influence cell differentiation, but few studies focused on the effect of the circularity of cell shape on the osteogenic differentiation of MSCs with a confined area during osteogenic process.

**METHODS:** In the present study, MSCs were seeded on a micropatterned island with a spreading area lower than that of a freely spreading area. The patterns had circularities of 1.0 or 0.4, respectively, and areas of 314, 628, or 1256  $\mu\text{m}^2$ . After the cells were grown on a micropatterned surface for 1 or 3 days, cell apoptosis and F-actin were stained and analyzed. In addition, the expression of  $\beta$ -catenin and three osteogenic differentiation markers were immunofluorescently stained and analyzed, respectively.

**RESULTS:** Of these MSCs, the ones with star-like shapes and large areas promoted the expression of osteogenic differentiation markers and the survival of cells. The expression of F-actin and its cytosolic distribution or orientation also correlated with the spreading shape and area. When actin polymerization was inhibited by cytochalasin D, the shape-regulated differentiation and apoptosis of MSCs with the confined spreading area were abolished.

**CONCLUSION:** This study demonstrated that a spreading shape of low circularity and a larger spreading area are beneficial to the survival and osteogenic differentiation of individual MSCs, which may be regulated through the cytosolic expression and distribution of F-actin.

**Keywords** Micropattern · Spreading area · Cell shape · Osteogenesis · F-actin

## 1 Introduction

Mesenchymal stem cells (MSCs) are widely distributed in the bone marrow, liver, fats, and other animal tissues [1]. They are pluripotent stem cells that self-renew and differentiate into osteoblasts, chondrocytes, adipocytes, and

myocytes [2]. The differentiation of MSCs into specific lineages appears to depend on their *in vivo* or *in vitro* exposure to local chemical and physical cues within their surrounding microenvironment [3, 4]. Cells can sense the adhesive features of substrates [4]; thus, some studies focused on the biological responses of MSCs cultured on micropatterned surfaces, particularly on osteogenic or adipogenic differentiation [5–7].

In the past two decades, some investigations have been implemented on the effect of cellular area and shape on the differentiation of MSCs [7–10]. For example, when hMSCs were cultured in rectangles of varying aspect ratios or fivefold symmetric shapes with an area of 2500  $\mu\text{m}^2$  and a

✉ Bo Huo  
huobo@bit.edu.cn

<sup>1</sup> Biomechanics Lab, Department of Mechanics, School of Aerospace Engineering, Beijing Institute of Technology, No. 5 South Zhongguancun Street, Beijing 100081, People's Republic of China

circularity of 0.84, 0.88, or 0.61 (circularity =  $4\pi \times \text{area}/\text{perimeter}^2$ ), the osteogenic differentiation of MSCs decreased monotonously with the increase in circularity [8]. When the circularity of cellular shape was 1, 0.785, 0.604, or 0.216 with the same adhesive area of  $900 \mu\text{m}^2$ , the adipogenic differentiation of MSCs increased monotonously with the increase in circularity, whereas their osteogenic differentiation showed the opposite trend [7]. In addition to cell shape, the spreading area of individual MSCs considerably influenced their differentiation. Adipogenic differentiation was mostly observed in the  $900 \mu\text{m}^2$  area, whereas osteogenic differentiation, in the  $3600 \mu\text{m}^2$  area [9]. A similar conclusion was obtained from another study, which showed that MSCs with large spreading areas ( $5026 \mu\text{m}^2$ ) have a higher tendency to differentiate into osteoblasts than MSCs with small spreading areas ( $1256$  or  $2827 \mu\text{m}^2$ ) [10].

The above studies revealed that spreading shape and area considerably influence MSCs differentiation, but no study considered both factors concurrently; therefore, many problems are still unexplained at present. For example, when the osteogenesis of bone marrow MSCs are initiated *in vivo*, the mineralized matrix or the degradation of adhesion molecules in osteoids may reduce the adhesion areas or constrain the adhesive shapes of MSCs [11]. Our previous studies showed that MC3T3-E1 osteoblasts confined in small circular patterns tend to differentiate osteogenically or undergo apoptosis, whereas a wrinkled shape with low circularity reduces the induced differentiation or apoptosis [12]. However, studies on the differentiation and apoptosis of MSCs with areas of less than  $1000 \mu\text{m}^2$  are rare.

Therefore, the present study aims to elucidate the effect of spreading shape on the differentiation or apoptosis of bone marrow MSCs with an area significantly smaller than the physiological value for simulating the *in vivo* crowded phenomenon in which MSCs still remain their differentiation capability. The micropatterning technique is adopted to fabricate the islands with different areas and circularities for seeding individual MSCs [12]. Then, the effect of spreading area and circularity on the osteogenic differentiation and apoptosis of MSCs is observed. Furthermore, the expression and intracellular distribution of F-actin and  $\beta$ -catenin are measured and analyzed to clarify the mechanism of cellular morphology-induced differentiation of MSCs.

## 2 Materials and methods

### 2.1 Surface fabrication

Two types of patterns, that is, circle and star were designed. The patterns had circularities of 1.0 and 0.4, respectively, and areas of 314, 628, or  $1256 \mu\text{m}^2$ . The parameters of the patterns are shown in Table 1. The

typical spreading area of MSCs on unpatterned surfaces is about  $2500 \mu\text{m}^2$ ; we used confined spreading area in this study. These patterns were replicated on a polydimethylsiloxane stamp via the procedure introduced in our previous papers [12–15]. The hydrophilization of the stamp was achieved by sputtering oxygen ions on its surface with an SBC-12 ion sputter coater (KYKY Technology Company, Beijing, China). The non-adhesive comb polymer purchased from Suzhou Nanotechnology Institute of CAS, which remained stable for approximately three months, was used [16]. Briefly, one droplet of the comb polymer solution was placed on the stamp surface and was made uniform by centrifugation at 1500 rpm. Finally, the stamp was gently pressed onto a culture dish for 10 s before the designed patterns were transferred onto the disk surface.

### 2.2 Cell culture

GIBCO Mouse (C57BL/6) bone marrow MSCs were purchased from Invitrogen and were cultured in an  $\alpha$ -minimum essential medium (Hyclone, Logan, UT, USA) supplemented with 10% fetal bovine serum (Gibco, Grand Island, NY, USA) plus 1% penicillin and streptomycin (Hyclone, Logan, UT, USA) at  $37^\circ\text{C}$ . We did not use an osteogenic induction medium to study the exclusive effects of spreading shape on MSC differentiation. The cells were seeded on micropatterned culture dishes at a density of  $5 \times 10^3$  cells/cm<sup>2</sup>, so that a single cell could attach to one adhesive region. After 30 min, the culture dish was gently washed to remove unattached cells. In the group for disrupting cytoskeleton, the seeded cells were cultured in a medium with  $1 \mu\text{g mL}^{-1}$  cytochalasin D (CD, Aladdin, Shanghai, China) for 24 h to inhibit actin polymerization.

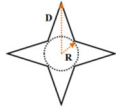
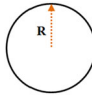
### 2.3 Apoptosis assay

One-step TUNEL Apoptosis Assay Kit (Beyotime, C1088, Shanghai, China) was used to detect the apoptosis of micropatterned MSCs. After treatment with 4% paraformaldehyde, cells were permeabilized with 0.3% Triton X-100 for 5 min at room temperature and then incubated with a TUNEL reaction mixture of the label solution for 60 min at  $37^\circ\text{C}$  in a humidified atmosphere in the dark, which was followed by rinsing with PBS. The cell nuclei were additionally counterstained with 0.1% Hoechst stain in PBS in the dark for 10 min. During observation under a fluorescence microscope, the cells in apoptosis revealed green fluorescence at nuclear regions.

### 2.4 Differentiation and $\beta$ -catenin measurements

After the cells were grown on a micropatterned surface for 3 days, they were gently washed with PBS, fixed with 4% paraformaldehyde in PBS for 30 min at room temperature,

**Table 1** Geometric parameters of the designed patterns

Shape	R ( $\mu\text{m}$ )	D ( $\mu\text{m}$ )	Designed area ( $\mu\text{m}^2$ )	Pattern's real area ( $\mu\text{m}^2$ )	Circularity
	7	16	314	313.9	0.4
	10	23	628	627.9	
	14	33	1256	1255.9	
	10	–	314	314.2	1
	14	–	628	628.1	
	20	–	1256	1256.6	

and permeabilized with 0.2% Triton-X 100 in PBS for 10 min at room temperature. The cells were blocked with 5% bovine serum albumin (Boster, Wuhan, China) for 30 min, incubated with goat antimouse polyclonal antibodies against alkaline phosphatase (ALP), type I collagen (COL I), or osteocalcin (OCN; Santa Cruz Biotechnology, Inc., Santa Cruz, CA, USA) at a 1:100 dilution for 60 min at 37 °C, then washed with PBS three times, and finally incubated in the dark for 60 min with an FITC-labeled affinity-purified antibody to goat IgG (Invitrogen, Carlsbad, CA, USA) at a 1:1000 dilution. The staining method of  $\beta$ -catenin (CST, 8480S, Boston, MA, USA) was the same as above.

## 2.5 F-actin measurements

After the cells were grown on a micropatterned surface for either 1 or 3 days, they were fixed for 5 min in 3.7% formaldehyde solution in PBS and permeabilized with 0.2% Triton-X-100 in PBS for 10 min at room temperature. Then, the cells were stained with a 50 mg/mL FITC phalloidin conjugate solution (SIGMA, Philadelphia, PA, USA) in PBS for 40 min at room temperature.

## 2.6 Statistical analysis

All experiments were performed at least in triplicate, and at least 30 cells were measured for each group. The fluorescent intensity of individual cells was measured by ImageJ software. Data were presented as mean  $\pm$  standard deviation if not specifically claimed. One-way ANOVA with Tukey's post hoc analysis was performed to determine the statistically significant differences between the mean values of different groups ( $p < 0.05$ ).

## 3 Results

### 3.1 Spreading morphology of MSC on different micropatterns

MSCs were cultured on the micropatterned substrate for 1 day, and then the intracellular F-actin and nuclei were immunofluorescently stained as shown in Fig. 1. It can be seen that the individual MSCs were well constrained in either star-like or circular pattern with different spreading

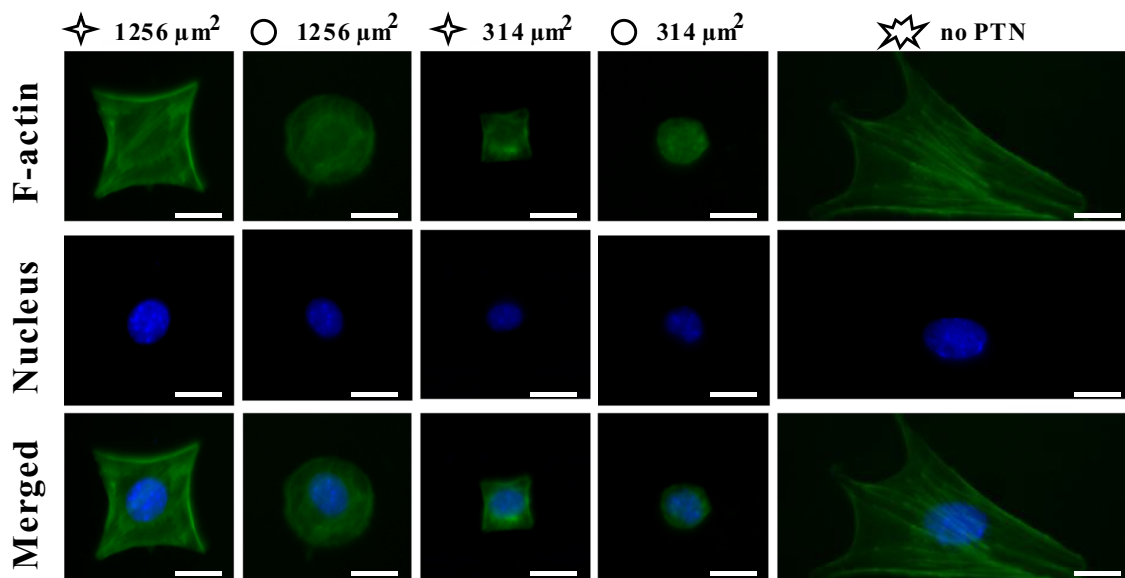
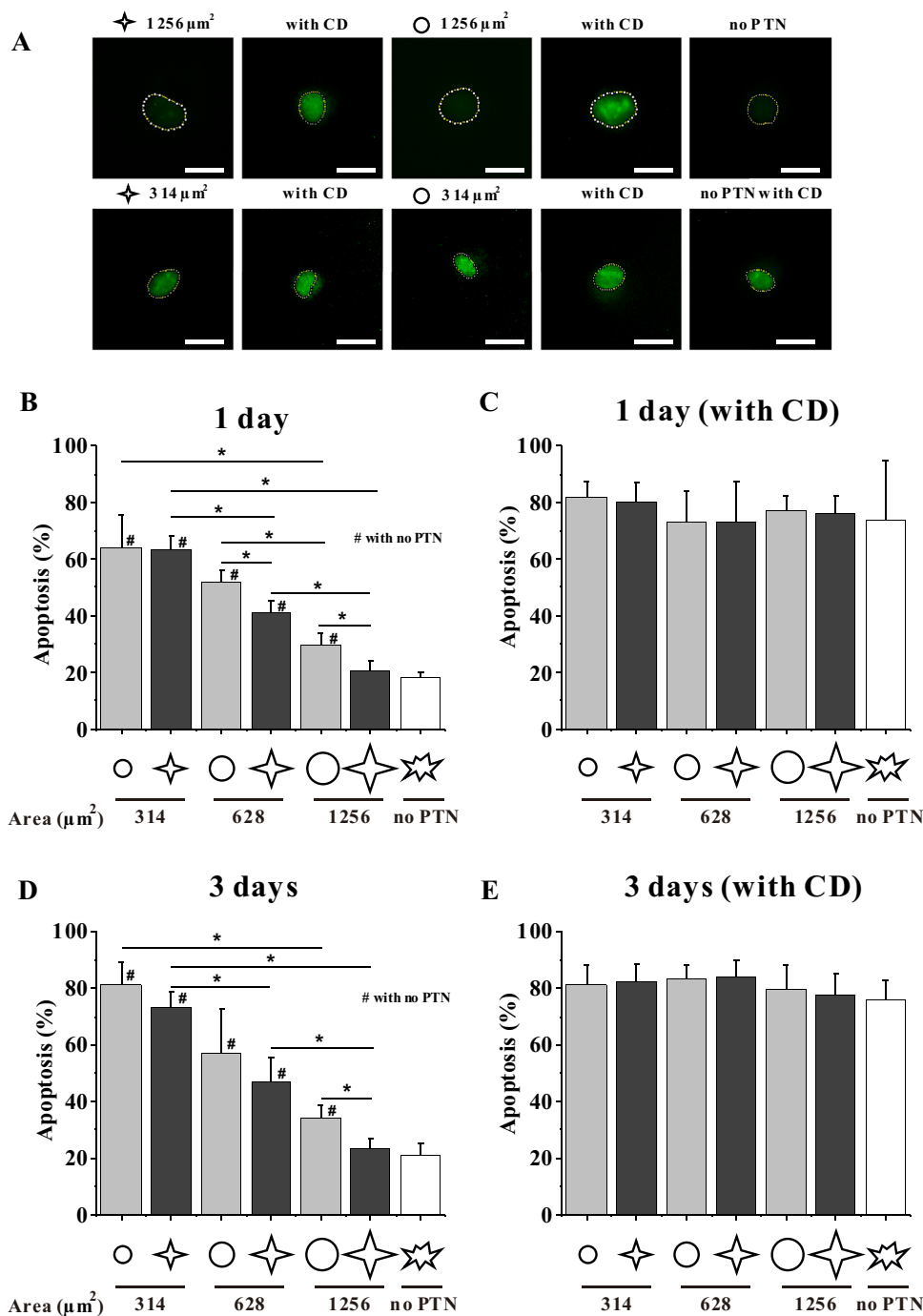


**Fig. 1** Fluorescent images of individual MSCs stained with FITC phalloidin for F-actin and with Hoechst for nucleus at 1 days after seeding. Scale bar, 20  $\mu\text{m}$

**Fig. 2** Effect of spreading shape and area on the apoptosis of MSCs. **A** TUNEL fluorescent images of MSCs cultured on circular or star-like patterns for 1 day. The dash lines indicate the nuclear contours. Scale bar, 20  $\mu\text{m}$ . **B–E** Statistical analysis of the apoptosis of MSCs on different patterns with or without CD for 1 or 3 days. \* $p < 0.05$



areas of 314  $\mu\text{m}^2$  and 1256  $\mu\text{m}^2$ , respectively, according to what we designed. Freely spreading MSCs (no-PTN) typically exhibit spindle or polygonal shape.

### 3.2 Spreading area and circularity determine the survival of MSCs

TUNEL assay was used to reveal the cells in apoptosis. The fluorescence images showed that TUNEL staining was observed in the nuclear region and the intensity was very

weak in no-PTN group but became stronger in patterned groups (Fig. 2A). The cells freely spreading on the culture plate could be regarded as alive, therefore the cells whose fluorescent intensity were higher than the mean nuclear intensity of freely spreading MSCs was considered as apoptotic. The statistical results showed that the smaller patterns of 314  $\mu\text{m}^2$  were not conducive to cell survival regardless of the shape and the apoptosis percentage reached up to 64% (Fig. 2B). With the increase of pattern area, the apoptosis percentage gradually decreased, e.g.

21% for  $1256 \mu\text{m}^2$  star-like cells that is similar to freely spreading cells. In addition, cell shape significantly influenced the apoptosis for  $628 \mu\text{m}^2$  and  $1256 \mu\text{m}^2$  MSCs, i.e. star-like pattern enhanced the survival of MSCs compared with circular pattern. After MSCs were cultured on the micropatterned substrate for 3 days, the apoptosis percentage of  $314 \mu\text{m}^2$  and  $628 \mu\text{m}^2$  cells obviously increased relative to 1 day, while that in the larger patterns or on blank surface remained unchanged, implying that the longer culture of MSCs in a confined environment promotes the apoptotic tendency (Fig. 2). The above results showed that cell shape, cell size and culture time regulate the survival of MSCs with confined adhesive morphology.

### 3.3 Spreading area and circularity regulate osteogenic differentiation of MSCs

Figure 3 shows the fluorescent images of FITC-labeled osteogenic differentiation markers, i.e. ALP, COL I, and OCN, and Fig. 4 presents their relative fluorescent intensity. After 3 days of seeding, the MSCs cultured on star

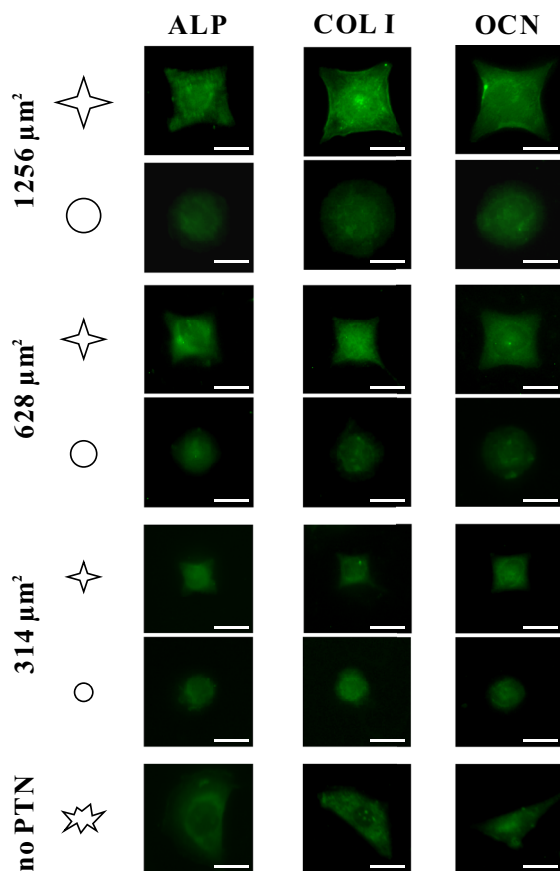


**Fig. 3** Fluorescent images showing the FITC-labeled protein expression of ALP, COL I, and OCN of individual MSCs cultured on the micropatterned regions and those on blank regions on the same slide for 3 days. Scale bar,  $20 \mu\text{m}$

islands expressed significantly higher levels of ALP, COL I, and OCN than those on circular islands (Fig. 4A, C, E). In addition, the MSCs on bigger islands of  $628$  or  $1256 \mu\text{m}^2$  had higher levels of fluorescent intensity of differentiation markers than those of  $314 \mu\text{m}^2$ . Therefore, the spreading shape and size of MSCs cooperatively regulate the osteogenic differentiation of MSCs.

### 3.4 Disruption of F-actin inhibits shape-induced apoptosis and differentiation

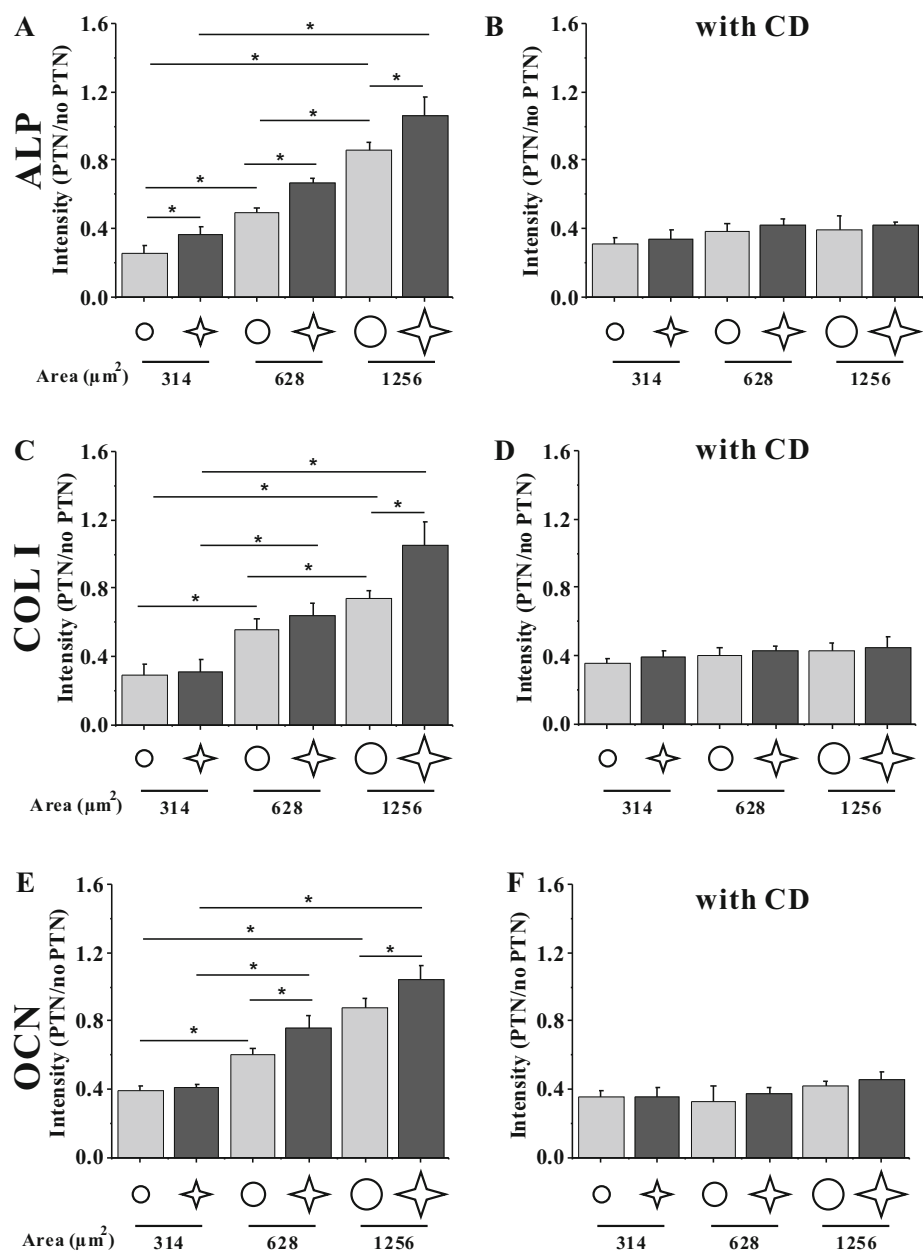
In this study, CD was used to inhibit the polymerization of actin monomers to investigate the relationship between cytoskeleton and the survival or differentiation of MSCs. After CD treatment, the spreading area of micropatterned or unpatterned cells obviously shrank (Fig. 5). After MSCs were cultured with CD for 1 day or 3 days, the TUNEL fluorescence intensity in the nuclei of star or circular  $1256 \mu\text{m}^2$  MSCs and freely spreading MSCs was significantly higher than that without CD treatment (Fig. 2A). The statistical analysis showed that CD caused nearly 80% apoptosis for micropatterned and unpatterned MSCs (Fig. 2C, E). For osteogenic differentiation, the shape-dependent expression of three markers was also reduced after F-actin was disrupted (Fig. 4B, D, F). These results suggested that the spreading shape-dependent apoptosis and differentiation of MSCs are strongly related to cytoskeleton structure.

### 3.5 Structure of F-actin is regulated by spreading area and circularity

To study the relationship between spreading area or shape and cytoskeleton further, we performed statistical analyses on the fluorescence images of F-actin. Results showed that when cells were cultured on  $1256 \mu\text{m}^2$  patterns for 1 day, F-actin was assembled on the star islands better than that on circular patterns (Fig. 1). When the area of MSCs was decreased, the intensity of F-actin was gradually reduced until it was significantly lower than that on unpatterned substrates (Fig. 5B). For the 3-day culture, MSCs on star-like islands of  $1256 \mu\text{m}^2$  had a significantly higher level of F-actin than those for 1-day culture or on other patterns (Fig. 5D). Moreover, MSCs on the smaller cell area or with longer culture time had a lower level of F-actin than those on unpatterned surfaces. After adding CD, no difference was found for MSCs on the patterns regardless of cell area, cell shape, and culture duration (Fig. 5C, E).

Since the cytoskeleton could generate mechanical forces and gets involved in cell adhesion, it is generally regarded that the arrangement of stress fibers might have a relationship with the cytoskeleton force, which can be revealed by coherency of F-actin [8, 17, 18]. The results of F-actin

**Fig. 4** A–F Statistical analyses of relative fluorescent intensity of the differentiation markers of MSCs without and with CD at 3 days after seeding. \* $p < 0.05$



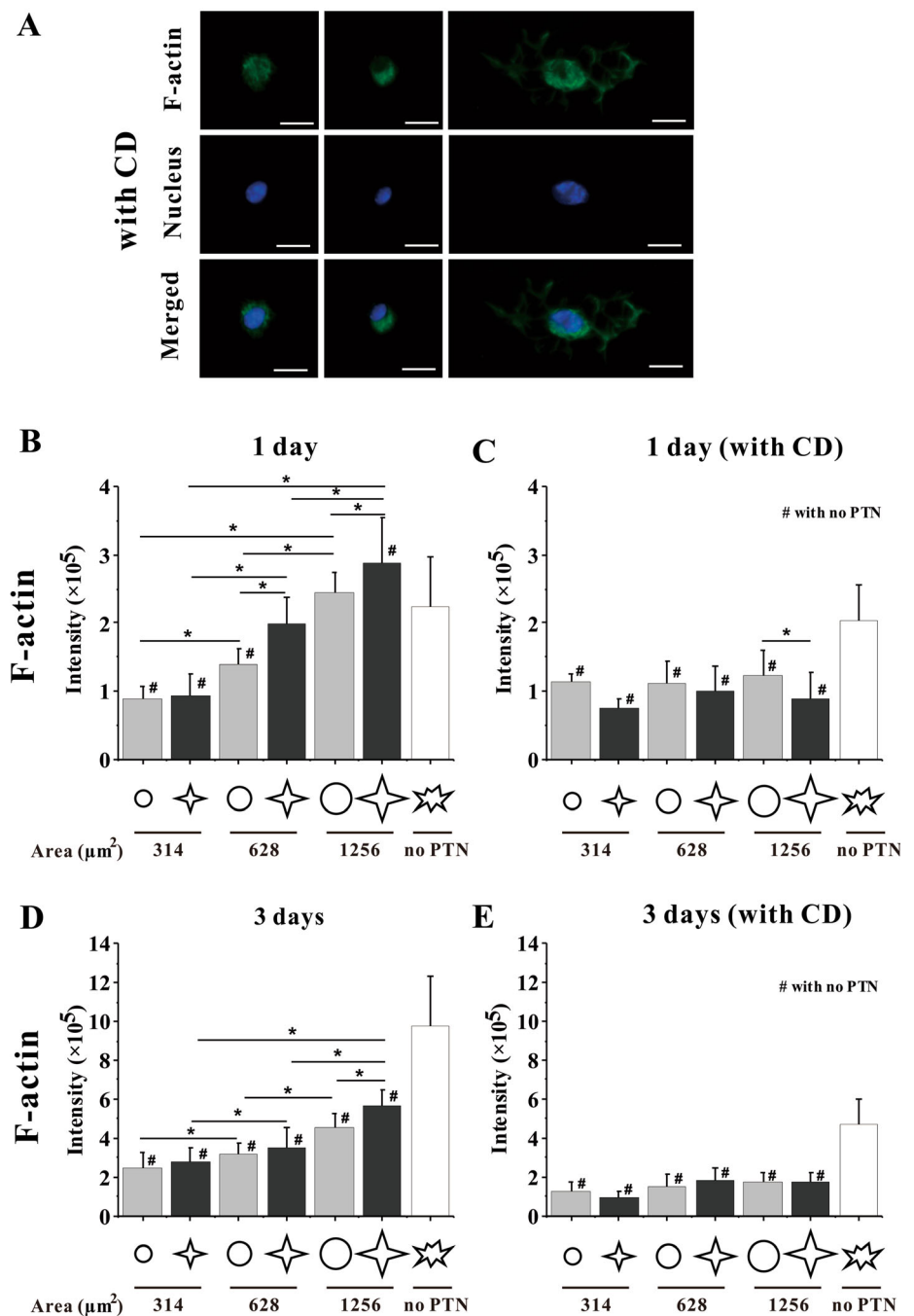
conformance analysis showed that the coherence of F-actin in circular-shaped cells cultured for 1 day was significantly lower than that of star-shaped cells, but both were lower than the no-PTN group (Fig. 6). After the 3-day culture, circular-shaped cells showed no significant difference with that of 1-day culture, whereas the coherence of F-actin in star-shaped cells was higher than the no-PTN group (Fig. 6C). After adding CD, no significant difference was observed between the patterned and control groups (Fig. 6B, D).

To explore whether osteogenic differentiation may be regulated by intracellular cytoskeletal distribution, we analyzed the distribution of F-actin in the cytoplasm and

nucleus, respectively. Figure 7 showed that when MSCs were cultured for 3 days, a higher level of F-actin in the cytoplasm or nucleus was found on the bigger star pattern of  $1256 \mu\text{m}^2$ . After decreasing the spreading area, the F-actin level in the cytoplasm or nucleus also decreased. Comparing the ratio of nuclear F-actin to cytoplasmic F-actin, the ratio was found to increase with the decrease in cell area, and the star-like pattern had a smaller value compared with the circular pattern, indicating that transferring F-actin from the cytoplasm to the nucleus may inversely correlate with the osteogenesis of MSCs (Fig. 7E). After culturing cells with CD for 3 days, the



**Fig. 5** Fluorescent images and statistical analyses of F-actin. **A** Fluorescent images of individual MSCs stained with FITC phalloidin for F-actin and with Hoechst for nucleus at 1 days after seeding with CD. Scale bar, 20  $\mu\text{m}$ . **B–E** The expression of F-actin in MSCs. Statistical analyses on the fluorescence intensity of F-actin in MSCs on different patterns without and with CD after 1-day seeding and 3-day seeding. \*, # $p < 0.05$



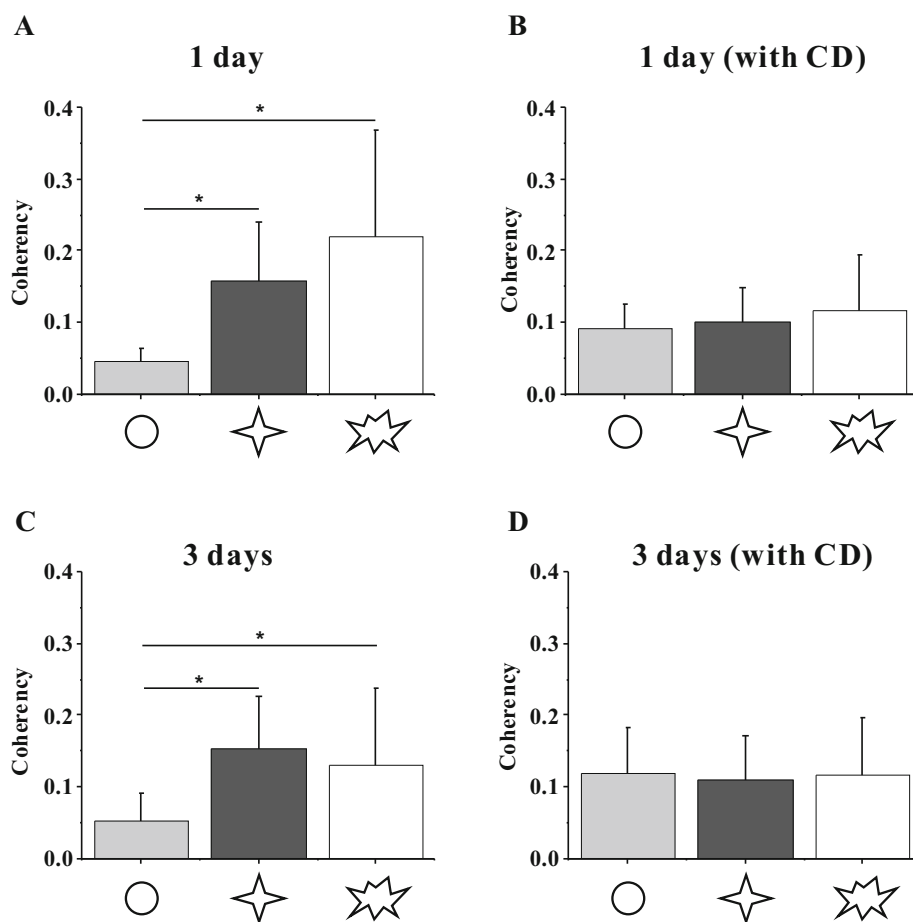
intracellular distribution of F-actin was independent of cell shape or area (Fig. 7C, D).

### 3.6 Intracellular distribution of $\beta$ -catenin is involved with spreading area and circularity

The physical properties of substrates regulate the Wnt signaling pathway [19–21]. To detect whether a micropatterned culture of MSCs initiates the Wnt pathway, we measured the expression and distribution of  $\beta$ -catenin,

the marker protein of the canonical Wnt signaling pathway (Fig. 8). The results of immunofluorescence staining after a 3-day seeding suggested that MSCs with a higher area or lower circularity expressed a higher level of  $\beta$ -catenin (Fig. 8C). After analyzing the ratio of  $\beta$ -catenin in the cytoplasm to that in the nuclear region, a significant difference was found only between MSCs on the large star island of 1256  $\mu\text{m}^2$  and those of 314  $\mu\text{m}^2$  (Fig. 8E). Adding CD in the culture medium reduced the difference

**Fig. 6 A–D** Orientation of F-actin in MSCs. Statistical analyses on the coherency of F-actin in MSCs on different patterns without and with CD after 1-day seeding and 3-day seeding. \* $p < 0.05$



of  $\beta$ -catenin expression among different groups (Fig. 8D, F).

#### 4 Discussion

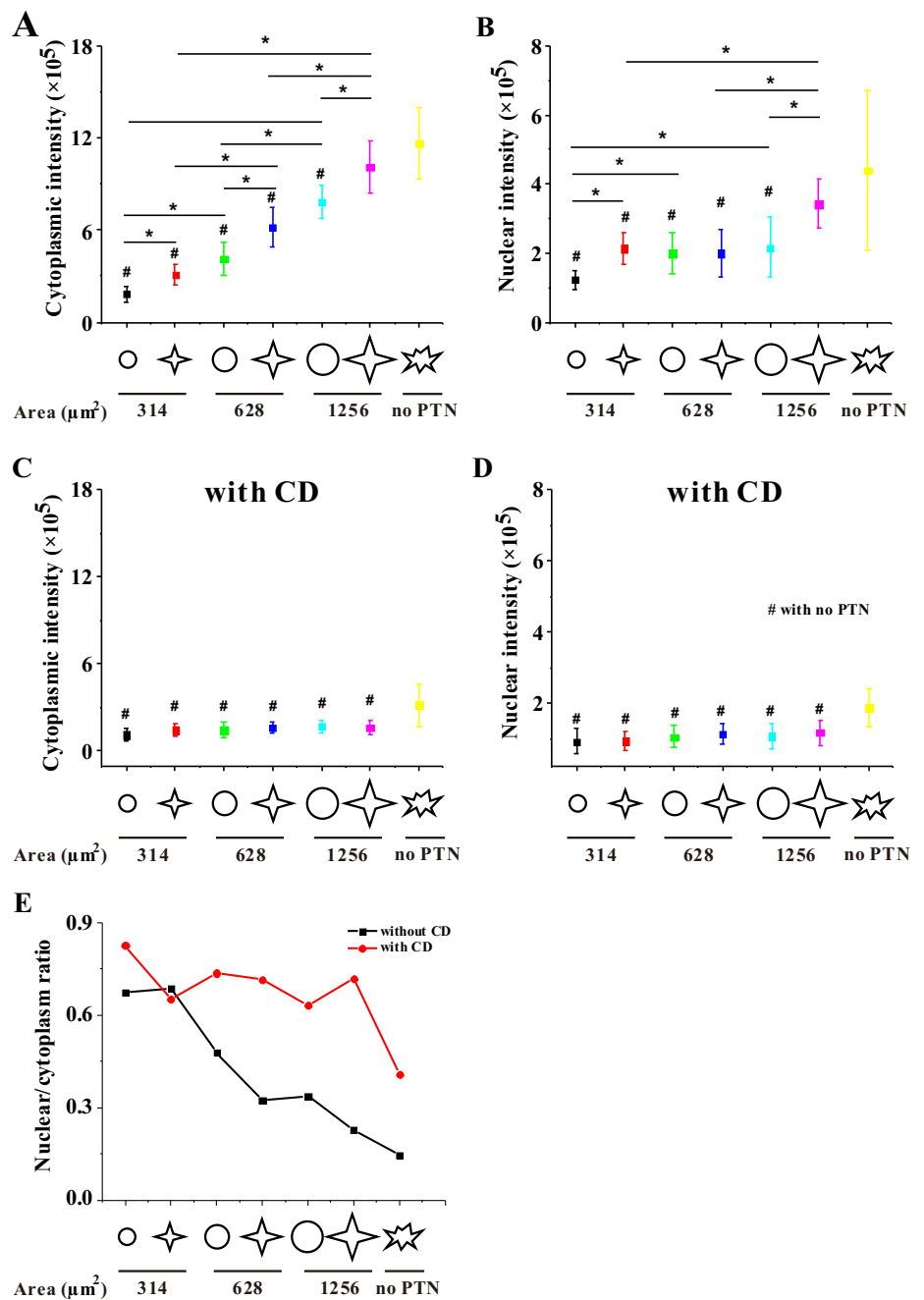
In the present study, the influence of geometric cues of single MSCs on their apoptosis and differentiation was investigated. Based on the fluorescent images of the cytoskeleton (Fig. 1), the micropatterned features constrained the boundary of MSCs. In this study, MSCs were found to grow abnormally on smaller patterns and tended to enter into apoptosis (Fig. 2A). As the spreading area of MSCs was increased, the degree of cellular apoptosis decreased. Moreover, star-shaped cells had a low level of apoptosis and were better for survival than circular ones especially with large areas (Fig. 2B, D). The probable reason was that the star-like geometry might be similar to the physiological shape of MSCs, implying that the spreading shape with lower circularity is more beneficial to the survival of MSCs. After CD treatment, most of cells entered into apoptosis regardless of spreading area and shape and there was no significant difference among

different groups (Fig. 2C, E). Therefore it was reasonably speculated that cytoskeleton played an important role in the adhesion and survival.

The current results on the osteogenic differentiation of MSCs showed that the expression levels of ALP, COL I, and OCN reveals their cell area- and shape-dependent tendencies (Fig. 4A, C, E). Large islands with low roundness promoted the expression of osteogenic markers, thus facilitating the osteogenesis of MSCs. By contrast, the circular cells tended to keep their original cell lineage. This result was similar to some previously reported findings that MSCs were more likely to differentiate into osteoblasts when the circularity of cell spreading area was small [7, 8]. This phenomenon seems to reveal that a trade-off occurs between apoptosis and differentiation; as the osteogenic differentiation of MSCs is strengthened, the apoptosis would be weakened. However, when rupturing the cytoskeleton of MSCs with CD, the cell roundness-regulated apoptosis or differentiation disappeared (Figs. 2C, E, 4B, D, F). These results indicated that the cytoskeleton might play important roles in the biological activities of cells.



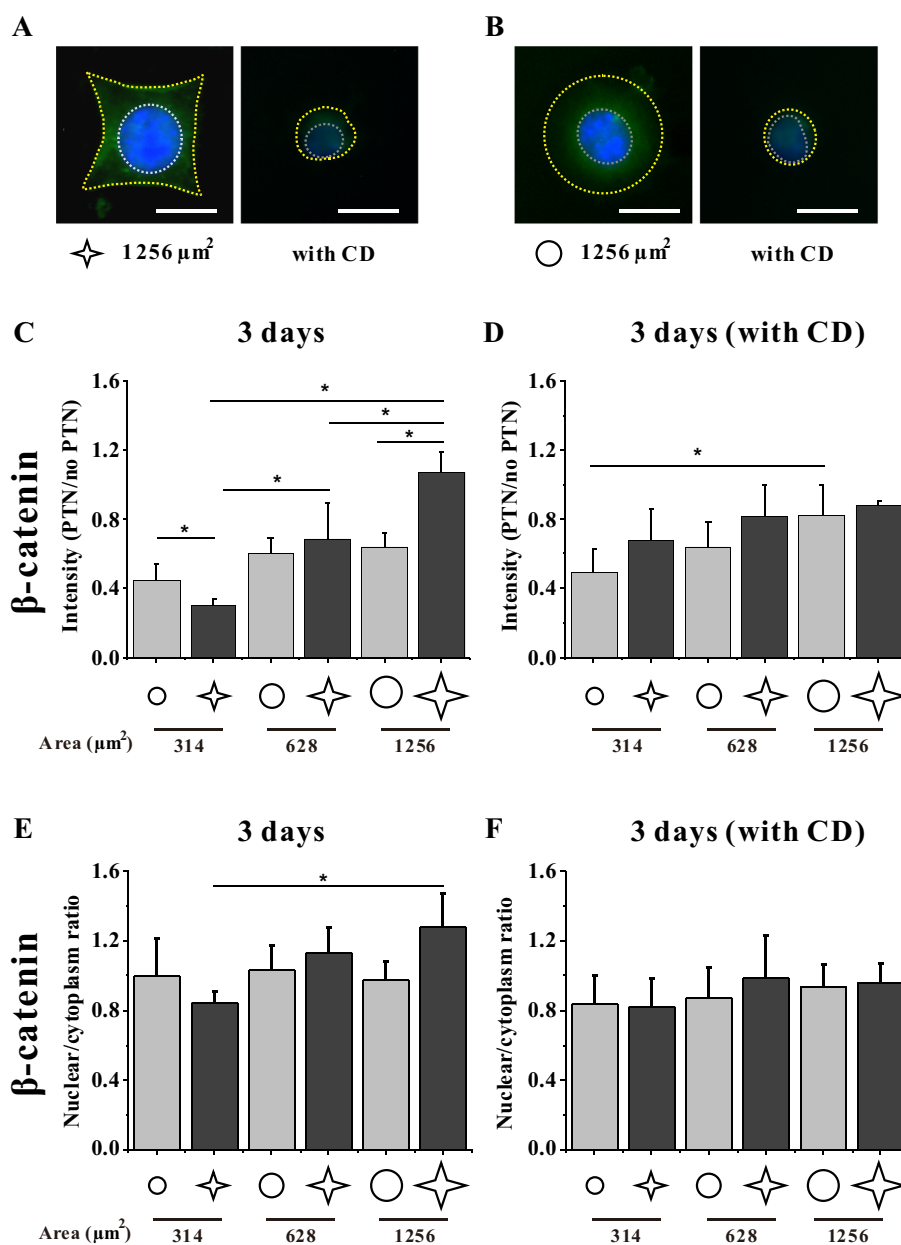
**Fig. 7** Statistical analyses on the distribution of F-actin in MSCs without and with CD after 3-day seeding. **A–D** Fluorescence intensity of F-actin in MSCs in the cytoplasm and in the nucleus. **E** Ratio of fluorescence intensity of F-actin in the nucleus to that in the cytoplasm. \* $p < 0.05$



To verify the cytoskeletal structure of MSCs during osteogenic differentiation induced by cellular area or shape, the fluorescent images of F-actin were analyzed in this study. The MSCs cultured on a star-like pattern of 1256  $\mu\text{m}^2$  predominately assembled actin filaments along the peripheral edges of the patterns and had strong actin filaments and stress fibers at the peripheral and central regions, which is similar to the freely spreading cells (Fig. 1). The statistical analysis about the coherency of F-actin revealed that the wrinkled shape of MSCs could increase the ordered assembly of the cytoskeleton (Fig. 6A,

C). This shape-dependent cell apoptosis or differentiation is due to the cytoskeleton remodeling playing a key role in both processes. When MSCs were constrained in the area of 314  $\mu\text{m}^2$ , which is obviously smaller than physiological area, the lack of adhesion space makes it difficult for cells to assemble their cytoskeleton. Increasing the area or peripheral ruffle of MSCs enhanced the assembly of F-actin and promoted the expression of osteogenic differentiation markers, suggesting that the highly assembled cytoskeleton may promote the osteogenic differentiation of MSCs. However, when cells were treated with CD for 1 day or

**Fig. 8** Distribution of  $\beta$ -catenin in MSCs without and with CD after 3-day seeding. **A**, **B** Fluorescence images of individual MSCs stained with FITC-labeled  $\beta$ -catenin. Scale bar, 20  $\mu$ m. The yellow and white dash lines indicate the cellular and nuclear contours, respectively. **C–F** Statistical analyses on the relative fluorescence intensity of MSCs and the ratio of intensity in the nucleus to that in the cytoplasm. \* $p < 0.05$



3 days, the actin network would be broken, and the effects of the patterns' area and shape on F-actin intensity disappeared (Fig. 5C, E), indicating that the integrity of cytoskeleton maintains the physiological activity of cells. In addition, after CD treatment F-actin could not form stress fiber bundle (Fig. 5A, C, E) so that the intracellular distribution of F-actin might change. We analyzed the intensity of F-actin in cytoplasm and nucleus and found that the ratio of F-actin in nucleus and cytoplasm was higher in CD group than that in normal group for larger patterns (Fig. 7E). The above results implied that a highly oriented assembly of F-actin in the cytosol is necessary for the survival or osteogenic differentiation of MSCs.

The classical Wnt signaling pathway had been shown to promote osteogenic differentiation of stem cells, and when this pathway was activated, the protein  $\beta$ -catenin would be transferred from cytoplasm to nucleus [19]. To evaluate the effect of classical Wnt signals on cells cultured on the substrate with different roundness, we assayed the level of  $\beta$ -catenin protein inside MSCs without CD or treated with CD (Fig. 8C, D). The star pattern of 1256  $\mu$ m<sup>2</sup> induced  $\beta$ -catenin accumulation and promoted the transfer of  $\beta$ -catenin into the nucleus of MSCs (Fig. 8E), which may activate the Wnt signaling pathway. However, the mechanism of related gene expression and signaling pathways in the nucleus during the osteogenic differentiation of MSCs is still unclear, and further research should be performed.

In conclusion, this study demonstrated that a spreading shape of low circularity and a larger spreading area are beneficial to the survival and osteogenic differentiation of individual MSCs, which may be regulated through the cytosolic expression and distribution of F-actin. These findings give insights into the mechanism of bone remodeling and tissue regeneration.

**Acknowledgement** This work was supported by the National Natural Science Foundation of China [11572043 and 11372043 (BH)].

#### Compliance with ethical standards

**Conflict of interest** The authors declare that they have no conflict of interest.

**Ethical statement** There are no animal experiments carried out for this article.

#### References

- Pittenger MF, Mackay AM, Beck SC, Jaiswal RK, Douglas R, Mosca JD, et al. Multilineage potential of adult human mesenchymal stem cells. *Science*. 1999;284:143–7.
- Tran NT, Trinh QM, Lee GM, Han YM. Efficient differentiation of human pluripotent stem cells into mesenchymal stem cells by modulating intracellular signaling pathways in a feeder/serum-free system. *Stem Cells Dev*. 2012;21:1165–75.
- Wang YK, Yu X, Cohen DM, Wozniak MA, Yang MT, Gao L, et al. Bone morphogenetic protein-2-induced signaling and osteogenesis is regulated by cell shape, RhoA/ROCK, and cytoskeletal tension. *Stem Cells Dev*. 2012;21:1176–86.
- Abagnale G, Steger M, Nguyen VH, Hersch N, Sechi A, Jousen S, et al. Surface topography enhances differentiation of mesenchymal stem cells towards osteogenic and adipogenic lineages. *Biomaterials*. 2015;61:316–26.
- Wang X, Song W, Kawazoe N, Chen G. Influence of cell protrusion and spreading on adipogenic differentiation of mesenchymal stem cells on micropatterned surfaces. *Soft Matter*. 2013;9:4160–6.
- Song W, Lu H, Kawazoe N, Chen G. Adipogenic differentiation of individual mesenchymal stem cell on different geometric micropatterns. *Langmuir*. 2011;27:6155–62.
- Peng R, Yao X, Ding J. Effect of cell anisotropy on differentiation of stem cells on micropatterned surfaces through the controlled single cell adhesion. *Biomaterials*. 2011;32:8048–57.
- Kilian KA, Bugarija B, Lahn BT, Mrksich M. Geometric cues for directing the differentiation of mesenchymal stem cells. *Proc Natl Acad Sci U S A*. 2010;107:4872–7.
- Yao X, Hu Y, Cao B, Peng R, Ding J. Effects of surface molecular chirality on adhesion and differentiation of stem cells. *Biomaterials*. 2013;34:9001–9.
- Song W, Kawazoe N, Chen G. Dependence of spreading and differentiation of mesenchymal stem cells on micropatterned surface area. *J Nanomater*. 2011;2011:265251.
- Knothe Tate ML, Adamson JR, Tami AE, Bauer TW. The osteocyte. *Int J Biochem Cell Biol*. 2004;36:1–8.
- Fu R, Liu Q, Song G, Baik A, Hu M, Sun S, et al. Spreading area and shape regulate apoptosis and differentiation of osteoblasts. *Biomed Mater*. 2013;8:055005.
- Huo B, Lu XL, Costa KD, Xu Q, Guo XE. An ATP-dependent mechanism mediates intercellular calcium signaling in bone cell network under single cell nanoindentation. *Cell Calcium*. 2010;47:234–41.
- Huo B, Lu XL, Hung CT, Costa KD, Xu Q, Whitesides GM, et al. Fluid flow induced calcium response in bone cell network. *Cell Mol Bioeng*. 2008;1:58–66.
- Lu XL, Huo B, Chiang V, Guo XE. Osteocytic network is more responsive in calcium signaling than osteoblastic network under fluid flow. *J Bone Miner Res*. 2012;27:563–74.
- Ma H, Hyun J, Zhang Z, Beebe Jr TP, Chilkoti A. Fabrication of biofunctionalized quasi-three-dimensional microstructures of a nonfouling comb polymer using soft lithography. *Adv Funct Mater*. 2005;15:529–40.
- Shukla A, Slater JH, Culver JC, Dickinson ME, West JL. Biomimetic surface patterning promotes mesenchymal stem cell differentiation. *ACS Appl Mater Interfaces*. 2016;8:21883–92.
- Müller P, Langenbach A, Kaminski A, Rychly J. Modulating the actin cytoskeleton affects mechanically induced signal transduction and differentiation in mesenchymal stem cells. *PLoS One*. 2013;8:e71283.
- Hsu SH, Huang GS. Substrate-dependent Wnt signaling in MSC differentiation within biomaterial-derived 3D spheroids. *Biomaterials*. 2013;34:4725–38.
- Du J, Zu Y, Li J, Du S, Xu Y, Zhang L, et al. Extracellular matrix stiffness dictates Wnt expression through integrin pathway. *Sci Rep*. 2016;6:20395.
- McMurray RJ, Wann AK, Thompson CL, Connelly JT, Knight MM. Surface topography regulates Wnt signaling through control of primary cilia structure in mesenchymal stem cells. *Sci Rep*. 2013;3:3545.

**Publisher's Note** Springer Nature remains neutral with regard to jurisdictional claims in published maps and institutional affiliations.